A myiasis model for *Philornis torquans* (Diptera: Muscidae) and *Pitangus sulphuratus* (Passeriformes: Tyrannidae)

Leonardo López[a,b,*], Agustin Izquierdo[c], Darío Manzoli[d,b], Pablo Beldoménico[d,b], Leonardo Giovanini[a,b]

[a]*Research Institute for Signals, Systems and Computational Intelligence, Universidad Nacional del Litoral, Ruta Nacional No 168 - Km 472.4, Santa Fe, Argentina, fich.unl.edu.ar/sinc*
[b]*National Council of Scientific and Technical Research (CONICET), Av. Rivadavia 1917, Buenos Aires, Argentina, www.conicet.gob.ar*
[c]*Universidad Nacional de Entre Ríos (UNER),Ruta Prov. 11 Km.10 Oro Verde, Entre Ríos, Argentina, www.bioingenieria.edu.ar*
[d]*Instituto de Ciencias Veterinarias del Litoral (ICIVET),R.P. Kreder 2805, Esperanza, Santa Fe, Argentina, www.icivet.santafe-conicet.gov.ar*

Abstract

The genus *Philornis* comprises neotropical parasitic flies that parasites bird nestlings in their larval stage. The ecology of most species of these parasitic flies is largely unknown. Here we present an epidemiological model that describes the behavior of parasite and host populations. The model was validated with real data of nestlings of the bird community present in a 30*ha* area in Santa Fe, Argentina. It consists of two weakly coupled population models, one for the larval population and the other for the nestling population. It takes into account, among other things, the importance of age structure for both populations, the immune response rate on the host and larval survivor rate, the incidence of larval load on host death rate, along with others. This work present a simple and intuitive way to represent the behavior of this complex biological system and it is a good starting point for future studies.

Keywords: `Myiasis`, `Parasite`, `Host`, `Larva`, `Model`, `Epidemic`.

1. Introduction

Myiasis are parasitic diseases caused by larvae of dipterans. They may represent great economic losses for livestock industry (e.g. species of *Lucilia* [1]), public health concern (e.g. *Dermatobia hominis* [2]), or contribute to wildlife species declines (e.g. *Philornis downsi* [3]). The ecology of myiasis has singular aspects that need consideration. The majority of infectious agents wait passively the contact with their host (e.g. a nematode egg must be accidentally ingested when the host forages) or are transmitted by a vector (e.g. malaria is transmitted by mosquitoes). In the transmission of myiasis, the gravid female fly actively seek for the host its larvae will feed on, even over relatively long distances. The ecology of myiasis has not been approached through theoretical studies [4].

Mathematical models are very important for understanding the underlying mechanism behind a disease.They are synthesized upon assumptions about biological mechanisms influencing temporal and spatial characteristics of the parasite spread [5]. They make the model formulation transparent and unambiguous since all the assumptions used to build it must be defined from basic theoretical knowledge in order to properly address the mechanism comprised in the system [6]. Analysis and simulation of these models can identify important combination of parameters, essential aspects or variables of the model that allow either understand the infectious diseases and find potential ways and means to control it.

Anderson and May [7], define two types of parasites with different epidemiological characteristics. On one hand microparasites such as bacteria and viruses increase rapidly in number when introduced into a susceptible host and there is no advantage on considering the number of infective agents. In this case, compartmental models are traditionally used and individuals are classified into susceptible, infected or immunized populations. On the other hand,

*Corresponding author
URL: `l.lopez@conicet.gov.ar` (Leonardo López)

sinc(*i*) Research Center for Signals, Systems and Computational Intelligence (fich.unl.edu.ar/sinc)
L. López, A. Izquierdo, R. Manzoli, P. Beldoménico & L. Giovanini; "A myiasis model for Philornis torquans (Diptera: Muscidae) and Pitangus sulphuratus (Passeriformes: Tyrannidae)"
Ecological Modelling, Vol. 328, pp. 62-71, may, 2016.

macroparasites such as worms are parasitic species for whom reproduction usually occurs trough transmission of immature stages that pass from one host to the next. Host mortality and morbidity increase with the number of parasites [8]. In this kind of models is important to consider not only the prevalence of infection, the parasite burden and the whole distribution of parasites among hosts since fertility, mortality and behaviour of host population depend on parasites distribution among hosts. Reinfection process is an important event in the interaction of hosts and parasites [6, 8, 9]. In these studies, much about understanding of interactions between parasites and hosts is based on the models introduced by Anderson and May [7, 10]. The authors show the importance of host heterogeneity in the dynamics of host-parasite interaction. These models have been the basis of a large development of empirical and theoretical literature [6, 9, 11, 12, 13, 14]. Some of the factors considered in this kind of models are: *i)* seasonality [15], *ii)* multi-species and/or trophic levels [16], *iii)* immunity [17], *iv)* spatial structure and *v)* genetic diversity [9].

Philornis Meinert (Diptera: Muscidae) is a genus of flies that includes several parasites species, whose larvae parasitize bird nestling [18]. Most parasitic Philornis spp. cause subcutaneous myiasis, with burrowing larvae tenet feed on nestlings blood, tissue and fluids [19] (Figure 1). These parasites harm nestlings causing mortality, reduced fitness and grow [10, 20]. Philornis downsi was subject of extensive research because of its negative impact on Darwin's Finches. The larvae of P. downsi reside in the nest material and feed intermittently on blood of nestlings [21]. Recently, Philornis torquans has been object of of several studies because its documented negative impact on bird nestlings, which can have sublethal effects, nestlings death or even a complete brood loss [22, 23, 24, 25, 26, 27]. It is also an excellent model to study the ecology of myiasis [28]. These flies only parasite nestlings of wild birds, which remains in their nests for the whole period in which they are susceptible to be parasite. At the same time, the larvae do not migrate once they penetrate in the bird's integument. They develop underneath the point where they entered the skin, and they are easily identified. All this allows a very specific and sensitive diagnosis, providing detailed information from every single nestling present in a patch of forest, from the day they hatch until they fledge.

This paper introduces a mathematical model of Philornis larvae and Pitangus sulphuatus nestlings populations behaviour. The model is build upon two compartmental models, one for each population, coupled through a function that quantified the effect of larvae load on nestlings death rate. The effect of nestling growth process on larvae load is addressed trough the inclusion of age structure of nestlings population, which leads to a set of coupled delayed differential equations (DDE) in contrast to the ordinary differential equations (ODE) resulting from compartmental models. They represent an approximation of the population of both species. The parameters of the models were estimated using real data in combination with quasi-newton optimization methods. The importance of this approach lies mainly in the fact that, up to date, there are no mathematical models explaining the relationship between larvae that cause myiasis and their hosts. The paper is organized in the following way: *Section* 2 introduce the populations models justifying the implemented methodology trough the assumed hypotheses, including a brief review about the myiasis process and data processing; *Section* 3 provides the results of the implemented model, parameters optimization a global sensitivity analysis; conclusions are summarized in *section* 4; *section* 6 include descriptive graphics and figures corresponding to model's results and *Appendix A* include the parameters obtained in the optimization procedure.

2. Methods

2.1. The data

The data were collected in the nature reserve in the city of Esperanza, Santa Fe, Argentina (center $60°55'00''W$, $31°23'08''S$). Around 100 nests were revised during this process in order to collect the relevant data for the model. This data was aligned assuming that all nestlings birth happen at the same time in order to obtain the behavior of both populations (larvae and nestling) in a single brood cycle.

2.2. The Model

The life cycle of Philornis flies is little known, but there is some information about they larval and pupal periods. The larvae penetrate the skin of the host and then began to grow. The larval growth process can be divided in three stages defined by their size: L_1 (up to $4mm$), L_2 (from $4mm$ to $7mm$) and L_3 (larger than $7mm$). After penetrating the skin development from L_1 to L_3 takes approximately 4 to 6 days for *Philornis carinatus* [23]. Then, L_3 emerges and pupates within the nest material, which takes from 1 to 3 weeks [23]. There are several factors acting at different levels that affect the dynamics of *Philornis* abundance. At the individual level, the main driver of the parasitism are the

sinc(*i*) Research Center for Signals, Systems and Computational Intelligence (fich.unl.edu.ar/sinc)
L. López, A. Izquierdo, R. Manzoli, P. Beldoménico & L. Giovanini; "A myiasis model for Philornis torquans (Diptera: Muscidae) and Pitangus sulphuratus (Passeriformes: Tyrannidae)"
Ecological Modelling, Vol. 328, pp. 62-71, may, 2016.

species and the age of the host. At the micro-habitat level the main determinants of larval abundance are the average height of the forest, at the ecosystem level, the density of hosts and prior rainfall [28].

The model consist on two coupled sub-models, one for each population. The coupling between populations is modelled trough a function that quantified the effects of larvae load on nestlings death rate. The larval development time (approximately 6 days) is three time shorter than nestlings one (approximately 19 days). Therefore, at least two flies generations are incubated in a single nestling cycle. One unexpected behaviour detected in real data, showed in Figure 2, is the co-existence of larvae from different developmental stages at the same time. This phenomena can be explained by the following facts: *i)* larvae raise and fall from nestlings during the day, *ii)* multiple infestations at different times, and *iii)* migration of larvae from dead nestlings in the same nest. Another unexpected behaviour exposed by Figure 2 is the presence of unexpected variations of L_2 and L_3 larvae populations. The L_2 larvae population is smaller than L_1 population, however, unexpected rises in L_3 population can be seen around days 9 and 17. These changes may be produced by: *i)* disparity in the measure of data, *ii)* difficulties in distinguishing between larval periods, and *iii)* migration of larvae from dead nestlings into the same nest.

The model of larvae population comprises three coupled delayed differential equations that represent the evolution of larvae populations through the different stages ($L_1(t)$, $L_2(t)$ and $L_3(t)$). The larvae birth rate is modelled as an external input of L_1 population. Since there are two generations of flies of flies for each nestling cycle the external input is given by

$$\mathcal{F}_1(t) = k_1 e^{-(t-t_1)^2/2\sigma_1^2} + k_2 e^{-(t-t_2)^2/2\sigma_2^2}. \tag{1}$$

Each term of $\mathcal{F}_1(t)$ characterizes the birth rate of each fly generation. The parameters t_1 and t_2 are the time when the average of the generation is arriving, σ_1 and σ_2 typifies the time distribution of the larvae birth, and k_1 and k_2 is the maximum number of larvae per generation. In a similar way, the larvae income in L_2 and L_3 populations are modelled as external inputs with similar structure.

$$\begin{aligned} \mathcal{F}_2(t) &= k_3 e^{-(t-t_3)^2/2\sigma_3^2}, \\ \mathcal{F}_3(t) &= k_4 e^{-(t-t_4)^2/2\sigma_4^2}. \end{aligned} \tag{2}$$

Finally, the effect of nestling immune response on larvae development is taking into acount by including an interaction term ($\varepsilon I_r(t) L_i(t) \quad i = 1, 2, 3$) and a simple model of the immune response. It is a simple measure the amount of antibodies produced by the host. We assume a complete compatibility between antibodies and larvae, the parasite do not replicate inside the host and the mortality of larvae is caused by the immune response. The parameters ε and a describe efficiency and rate host immune response respectively. The resulting model is given by

$$\begin{aligned} \dot{L}_1(t) &= [1 - \mu_1 - \varepsilon I_r(t)] L_1(t) - \beta_1 L_1(t - \tau_l) + \mathcal{F}_1, \\ \dot{L}_2(t) &= [1 - \mu_2 - \varepsilon I_r(t)] L_2(t) - \beta_2 L_2(t - \tau_l) + \beta_1 L_1(t - \tau_l) + \mathcal{F}_2, \\ \dot{L}_3(t) &= [1 - \mu_3 - \varepsilon I_r(t)] L_3(t) - \beta_3 L_3 + \beta_2 L_2(t - \tau_l) + \mathcal{F}_3, \\ \dot{I}_r(t) &= \frac{a}{1 + e^{-(L(t)-\bar{L})/s}} I_r(t), \end{aligned} \tag{3}$$

where $L_1(t)$, $L_2(t)$ and $L_3(t)$ are the larvae population at different growth stages, $L(t) = L_1(t) + L_2(t) + L_3(t)$ is the total larvae load at time t, $\bar{L}$ is the mean larvae population and $I_r(t)$ is the intensity of the nestlings immune response. Table 1 compiles the biological meaning of each parameter and Figure 3 shows the block diagram that describes the larvae growth process.

The behaviour of nestlings populations can be characterized using a compartmental model. The nestling population is organized in three sub-populations: *i)* susceptible (S) are nestlings without larvae but sensitive to charge them, *ii)* infested (I) are nestlings with larvae and finally *iii)* removed (R) are nestlings that are move out of the nest. Analyzing the data collected we found that models relaying on homogeneous populations fail to describe the dynamic behaviour of sub-populations. This issue rises from the physiological and anatomical changes suffered by nestlings

Parameter	Description
μ_i	Natural death rate of L_i
β_i	Rate of passage of state L_i to L_j, with $i \neq j$
ε	Efficiency of the host immune response
a	Rate host immune response
$\mathcal{F}_i$	External supply of larvae at L_i
t_i	Mean time where the input is made
k_i	Scaling factors
σ_i	Standard deviation

Table 1: Larvae model parameters meaning

during their growth process. The skin of nestlings has no protection coverage (feathers) that make them more susceptible to larvae infestation when the broods just born, and for a couple of days. As the nestlings grow, they begin to develop the feathers that reduce their susceptibility to larvae and increase their survivability to infections. Finally, when nestlings complete their growth process are fully feathered and they are able of flying. Therefore, it is necessary to include information about the growing process into the model. This information is incorporated into the model by arranging the three sub-populations into three age groups that define the different developmental stages: *i)* newly born, *ii)* on development, and *iii)* fully developed. These stages, and the corresponding age groups, can be identified from the analysis of the evolution of anatomical characteristics(size, weight and tarsus) along the breading time. They show an exponential growth pattern

$$S(t) = S_{max}(1 - e^{-\tau_h t}), \tag{4}$$

where t is the development time of the brood, τ_h is the time when brood reaches 66% of the final value of the characteristic S_{max}. Figure 4 shows the evolution of the relationship weight/size along the breeding period. This pattern is consistent with the Von Bertalanffyt model [29] for $\tau_h = 6.3$ days. This way of modelling the nestling growth process allows to organize the susceptible and infested sub-populations into three groups according to their developmental stages: *i)* nestling whose age is bellow τ_h (groups S_1 and I_1) that characterize for a high susceptibility to larvae infestation (β_{H1}) and death rate (μ_{I1}), *ii)* nestlings whose age is between τ_h and $2\tau_h$ (groups S_2 and I_2) that characterize for a moderate susceptibility (β_{H2}) and death rate (μ_{I2}), and *iii)* nestlings whose age is older than $2\tau_h$ (groups S_3 and I_3) that shows low susceptibility (β_{H3}) and death rate (μ_{I3}). The resulting model for nestling population is given by

$$\begin{aligned}
\frac{dS_1}{dt} &= (b_{S_1} - \beta_{H1} - \mu_{S_1})S_1(t) + \gamma_1 I_1(t) - s_{12}S_1(t-\tau_h) + k\Gamma(t),\\
\frac{dI_1}{dt} &= \beta_{H1}S_1(t) + (b_{I_1} - \gamma_1 - \mu_{I_1})I_1(t) - i_{12}I_1(t-\tau_h),\\
\frac{dS_2}{dt} &= s_{12}S_1(t-\tau_h) + (b_{S_2} - \beta_{H2} - \mu_{S_2})S_2(t) + \gamma_2 I_2(t) - s_{23}S_2(t-\tau_h),\\
\frac{dI_2}{dt} &= i_{12}I_1(t-\tau_h) + (b_{I_2} - \gamma_2 - \mu_{I_2})I_2(t) + \beta_{H2}S_2(t)S_2 - i_{23}I_2(t-\tau_h),\\
\frac{dS_3}{dt} &= s_{23}S_2(t-\tau_h) + (b_{S_3} - \beta_{H3} - \mu_{S_3})S_3(t) + \gamma_3 I_3(t) - s_{3R}S_3(t-\tau_h),\\
\frac{dI_3}{dt} &= i_{23}I_2(t-\tau_h) + (b_{I_3} - \gamma_3 - \mu_{I_3})I_3(t) + \beta_{H3}S_3(t) - i_{3R}I_3(t-\tau_h),
\end{aligned} \tag{5}$$

where the function $\Gamma(t)$ represent the birth distribution along time and $\mu_i(L) \quad i = I_1, I_2, I_3$ models the death rate of corresponding populations. The gamma function is used to model the birth distribution since it is a function that can

assume a range of shapes, from exponential to normal, using only two parameters. The time distribution of nestlings birth is given by

$$\Gamma(t) = \frac{1}{\Gamma(c)\theta^c} t^{(c-1)} e^{(-t/\theta)}, \tag{6}$$

where the parameters c and θ control the scale and shape of the time distribution. The death rates of infected sub-populations I_1, I_2 and I_3 depend on the larvae load of each nestling. When the larvae load is below the average load $\bar{L}$, the death rate is low. However, when the larvae load is over $\bar{L}$, the death rate grows linearly with the load. Then, the death rate for I_1, I_2 and I_3 is given by

$$\mu_i(L) = \mu_0 + ln(1 + k_i e^{-(L-\bar{L})})) \quad i = I_1, I_2, I_3, \tag{7}$$

where μ_0 is the natural death rate and k_i is the sensitivity of the population. The biological meaning of the parameters (equations 6 and 7) is summarized in Table 2, here $i, j = 1, 2, 3$ and $i \neq j$. Figure 5 shows the block of the nestlings populations behaviour.

Parameter	Description
$\Gamma(\theta, c, t)$	Birth distribution function.
b_{S_i}	Rate at which susceptible individuals remains in susceptible state.
μ_{S_i}	Natural death rate.
b_{I_i}	Rate at which infected individuals remains in infected state.
τ_h	Growth delayed.
β_{Hi},	Infective rate.
γ_i	Recovery rate.
μ_{I_i}	Death rate by larval action.
s_{ij}	Pass rate from S_i to S_j
i_{ij}	Pass rate from I_i to I_j
s_{3R}	Immunization rate of feather of susceptible population
i_{3R}	Immunization rate of feather of infected population
k	Scaling factor.

Table 2: Nestlings model parameters meaning

Some important aspects to consider in this model are the parameters s_{ij} and i_{ij}, that represent the step rate from S_i to S_j and from I_i to I_j respectively. They are affected by the developmental time τ_h, as well as the step rate from infected or susceptible to removed i_{3R} and s_{3R}.

The final form of the model is shown in Figure 6, where the coupling between the larvae and nestlings models previously described and the relation between the nestlings and the larvae can be observed. The larval population affect trough the β_{Hi} parameter the nestlings population; due to the difference of development for both populations, larval population tends to accumulate at the second period of bird develop as we will see later in the Results section.

3. Results and discussion

The model parameters were estimated following a two stages optimization procedure: *i)* Firstly, a global search using stochastic optimization algorithms [30, 31] and then, *ii)* a local search using gradient based optimization algorithms [32, 33]. This procedure allows us to explore the entire space of parameters searching for good candidates

sinc(*i*) Research Center for Signals, Systems and Computational Intelligence (fich.unl.edu.ar/sinc)
L. López, A. Izquierdo, R. Manzoli, P. Beldoménico & L. Giovanini; "A myiasis model for Philornis torquans (Diptera: Muscidae) and Pitangus sulphuratus (Passeriformes: Tyrannidae)"
Ecological Modelling, Vol. 328, pp. 62-71, may, 2016.

(global search), which are used to find the best parameters for the model through a local search. The stochastic optimization methods provides good starting points for gradient-base optimization methods. The objective function used in these stages is the *Normalized Mean Square Error (NMSE)*, given by

$$NMSE = \sum_{i=1}^{3} \sum_{k=1}^{M} \frac{\| M_i(k) - D_i(k) \|_2^2}{\| M_i(k) \|_2^2}, \tag{8}$$

where $M_i(k)$ are the temporal dynamics obtained by the model and $D_i(k)$ are the temporal dynamics of real data.

The global search was performed using simulated annealing [34] with 1000 iterations and a stopping criteria of $1e-10$. The parameters obtained in this stage were used as a initial condition for the local search solved using a Quasi-Newton method with a cubic line search procedure in order to find the best estimation [35]. The objective function employed for estimating the parameters of larvae model was

$$NMSE_{larvae} = \sum_{i=1}^{3} \sum_{k=1}^{M} \frac{\| L_i(k) - \hat{L}_i(k) \|_2^2}{\| L_i(k) \|_2^2}, \tag{9}$$

where $\hat{L}_i(k)$ is the larval population predicted by the model; $L_i(k)$ is the real larval population and $i = 1, 2, 3$ corresponds to the larval type. The corresponding parameters are resumed in Table A.3. The objective function employed for estimating the parameters of the myiasis model was

$$NMSE_{myiasis} = \sum_{i=1}^{3} \sum_{k=1}^{M} \frac{\| S_i(k) - \hat{S}_i(k) \|_2^2}{\| S_i(k) \|_2^2} + \frac{\| I_i(k) - \hat{I}_i(k) \|_2^2}{\| I_i(k) \|_2^2}, \tag{10}$$

where $S_i(k)$ and $I_i(k)$ represent the real proportion of Susceptible and Infected population and $\hat{S}_i(k)$ and $\hat{I}_i(k)$ are the populations predicted by the model, with $i = 1, 2, 3$ indicating the developmental phase. The parameters obtained are shown in Table A.4.

Figure 7 shows the results of the adjusted temporal dynamics for L_1, L_2 and L_3 populations in the larval model. In general the model seems to correspond to the actual data processed and reliably represents the behavior of the population mean. It can be seen that the mortality of larvae L_1 seems to be greater than the other two types, this idea is supported by the parameters β_1 and μ_1, which is the rate of larvae that goes from L_1 to L_2 state and the death rate of L_1. On one hand, the value of β_1 is lower than β_2 and β_3, indicating that fewer larvae spend from L_1 to L_2. On the other hand, the value of μ_1 suggest that the mortality is bigger for larvae in the fist stage. Both L_1, as L_2 and L_3 temporal dynamics capture the different waves of larvae that affect the nestlings. L_1 temporal dynamic shows a well defined peak around the day 14, the L_2 temporal dynamic shows the stagnation and population decline of this larval stage by the factors explained above, the L_3 temporal dynamic shows two well defined peaks on day 9 and day 17. The low value obtained for ε and a, which indicates a low host immune response corresponds to the hypothesis that a lower immune response, the host receives a greater burden of larvae.

Figure 8 shows the results of the adjusted temporal dynamics for susceptible nestlings population (S_1, S_2 and S_3) and infested nestlings population (I_1, I_2 and I_3). It can be seen easily as the susceptible population decreases markedly from the first stage (S_1) to the last (S_3). Moreover, the population of infested nestlings remains almost constant throughout the parasitic process. This aspect is also reflected in the values of the set parameters (Table A.4), especially the β_{H2} and S_{12} which warns that it between the first and second stage of development when most infestation occurs in the population.

The nestlings model reflects a strong temporal aggregation of the three stages of development. The incidence of infection by the larvae appears to decrease as the nestling grows, this behavior of the model corresponds with the real data, as the individual develops acquires plumage that protects the larvae.

Parameters μ_{I1}, μ_{I2} and μ_{I3} confirm the hypothesis made about the death rate (equation 7), the greater the number of larvae is higher death rate. The parameter S_{3R} measure the rate of susceptible individuals that are removed from the final stage, this parameter is significantly bigger than I_{3R} i.e. the rate of infested individuals that are removed from the final stage, this corresponds with the idea that removed individuals from the last development stage are in fact recovered individuals and those individuals without larvae are more likely to fly.

sinc(*i*) Research Center for Signals, Systems and Computational Intelligence (fich.unl.edu.ar/sinc)
L. López, A. Izquierdo, R. Manzoli, P. Beldoménico & L. Giovanini; "A myiasis model for Philornis torquans (Diptera: Muscidae) and Pitangus sulphuratus (Passeriformes: Tyrannidae)"
Ecological Modelling, Vol. 328, pp. 62-71, may, 2016.

3.1. Global Sensitivity Analysis

Global Sensitivity Analysis (GSA) describes a set of mathematical techniques to know how the variation in the output of a mathematical model can be attributed to variations of its parameters. GSA can be applied for multiple purposes, such as to investigate the relative influence of the parameters over the predictive accuracy of the model in order to simplify, calibrate and validate the model using experimental data. To perform GSA of the model proposed in this work, we use the SAFE toolbox [36]. In this toolbox two well established variance-based sensitivity indexes are implemented:

- the first-order sensitivity index or 'main effects'.
- the total-order sensitivity index or 'total effects'.

The variance-based first-order indices ('main effects') and total-order ('total effects') indices [37] were computed using an approximation technique [38].

For the analysis of the Philornis model, the parameters that are not strictly defined by biological factors of the Philornis population were analyzed by computing both sensitivity indexes (first-order and total-order). The parameters included in this analysis were: the natural death rate μ_i; $i = 1, 2, 3$, the transition rate from L_i to L_j , β_i ; $i, j = 1, 2, 3$ and $i \neq j$, the efficiency of the host immune response ε and the rate of hots immune response a. The other parameters of this block are fixed by the natural cycle of the fly and they do not change from one cycle to another.

The number of uncertain parameters that are allowed to vary in this analysis, M, is eight: μ_i, β_i, ε and a. The parameters employed in the analysis were computed using an uniform distribution function given by $[X_i - \delta_i,\ X_i + \delta_i] \quad i = 1, ..., 8$ and $\delta = 0.1$, that is, a variation of 10% of the studied parameters. The sample size N was fixed to 1000, such that the total number of model evaluations was 10000.

Figure 9 shows the sensitivity indices for the larvae model parameters. For simplicity, only the most relevant ones are showed (those which showed greater variability). The main effect sensitivity analysis and the total effect sensitivity analysis shows the influence of μ_2 and β_2 in the model behavior. These parameters determine the dynamics of the L_2 larvae stage, the death rate and the pass to L_3 respectively. In the case of the total effect indices, it ca be seen how the variation of all the parameters at the same time affect in a more significant way the behaviour of the model, and again μ_2 and β_2 are the ones that induce more uncertainty.

Figure 10 compares the best set of parameters of the GSA, when the the main effect and total effect sensitivity indices vary less; the worst case, when the the main effect and total effect sensitivity indices vary more; the model case, or the set of parameters obtained in the optimization process, and the real data. This figure shows that even when the variation of the parameters appear to affect the sensitivity of the model in a significant way, this variation does not produce a very different response in the model temporal dynamics. Even in the worst case the obtained temporal dynamics seems to be reasonable compared with the adjusted model and the real data.

For the analysis of the nestlings population we study the effect the following parameters: natural death rate μ_{S_i} $i = 1, 2, 3$, death rate by larval action μ_{I_i} $i = 1, 2, 3$, infective rate β_{H_i} $i = 1, 2, 3$ and recovery rate γ_i $i = 1, 2, 3$. The other parameters are determined by the biology of the nestlings. Here, the number of uncertain parameters that are allowed to vary, M, is twelve: μ_{S_i}, μ_{I_1}, β_{H_i} and γ_i. The parameters employed in the analysis were computed using an uniform distribution function given by $[X_i - \delta_i,\ X_i + \delta] \quad i = 1, ..., 12$ and $\delta = 0.1$. The sample size N was fixed to 1000, such that the total number of model evaluations was 10000.

Figure 11 shows the sensitivity indices of the nestling model parameters. Again, only the more sensitive parameters are showed. The convergence of the model seems to be most affected when the parameters vary at the same time, as shows the total effect indices. However, from both, main and total effect can be seen that β_{H2} and μ_{I_2} strongly affect the convergence. These parameters describe infection and death rates of nestlings that are in the second developmental stage. This figure shows that parameters that most affect the sensitivity of the model are those related to the infection and death rates of infected nestlings.

Figure 12 shows the comparison for the best set of parameters of the GSA, when the the main effect and total effect sensitivity indices vary less; the worst case, when the the main effect and total effect sensitivity indices vary more; the model case, or the set of parameters obtained in the optimization process, and the real data for the nestlings model. Again, as well as in the case of the Philornis model, the temporal dynamics obtained are very similar for the best and the worst case compared with the adjusted model, showing the robustness of the model. Even in the worst case,

the temporal dynamics are very similar to those obtained in the adjustment process with a decrease in the infected nestlings.

4. Conclusions

The Philornis gender is considered a generalist parasite group of birds, it means they use a host independently of his characteristics nest material. In the other hand, the impact of this parasites on the local birds species and in general fauna is a trend topic due to the great economic losses induced by myiasis in domestic animals breeding, as well as public health problems and of curse, local fauna population decay. In this order extremely important to have a model that replicates the process dynamics.

In this paper we have made a first step in order to contribute to understand the myiasis process, introducing an extended host-parasite model which replicate close enough the real dynamic of a myiasis process in a wild population of birds opening the scene for more complex models that contemplate different assumptions inherent to more specific problems. The separation of population in three development stages was an successful strategy because the main parameters that control the model are affected by the age of the brood.

The model was able to corroborate the proposal hypothesis about the relationship between parasite load and nestlings mortality. It shows that the number of larvae and death rate of the host population are directly related. Beyond a certain threshold, the death rate tends to increase linearly. Furthermore, the host immune response tend to affect the death rate of larvae and the survival rate of the host, it depends on the parasite load of the host, and the rate of the host immune response. As it requires certain metabolic costs, the model considers them through a threshold. The low rate in the host immune response and the relatively low mortality of the host population make favorable the relationship between this two population, justifying the results with field observations.

The Global Sensitivity Analysis shows that critical parameters of each model do not vary significantly, while Figures 9 and 11 show variability in indices rates, this variability is nos significant if it is taken into account the scale of the Figures. On the other hand, the temporal dynamics for both models seems to fit very well even for the worst set of parameters resulting of the GSA.

In a future work the model will be employed to analyze the behaviour of myiasis on other host populations(Phacellodomus sibilatrix or Phacellodomus ruber), in order to compare the impact of parasite. A more detailed analysis of the model parameters i.e. stability analysis is the topic for a future paper.

5. Acknowledgements

The authors wishes to thank: the *Universidad Nacional del Litoral* (with CAID 501 201101 00548 LI), and the *Consejo Nacional de Investigaciones Científicas y Técnicas* (CONICET) from Argentina, for their support.

sinc(*i*) Research Center for Signals, Systems and Computational Intelligence (fich.unl.edu.ar/sinc)
L. López, A. Izquierdo, R. Manzoli, P. Beldoménico & L. Giovanini; "A myiasis model for Philornis torquans (Diptera: Muscidae) and Pitangus sulphuratus (Passeriformes: Tyrannidae)"
Ecological Modelling, Vol. 328, pp. 62-71, may, 2016.

6. Images

Figure 1: Nestling infested with larvae.

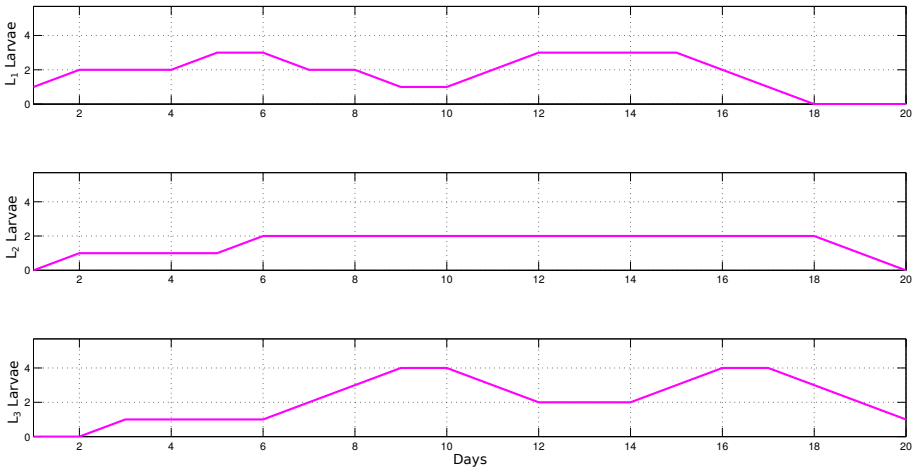

Figure 2: Aligned larvae population.

sinc(*i*) Research Center for Signals, Systems and Computational Intelligence (fich.unl.edu.ar/sinc)
L. López, A. Izquierdo, R. Manzoli, P. Beldoménico & L. Giovanini; "A myiasis model for Philornis torquans (Diptera: Muscidae) and Pitangus sulphuratus (Passeriformes: Tyrannidae)"
Ecological Modelling, Vol. 328, pp. 62-71, may, 2016.

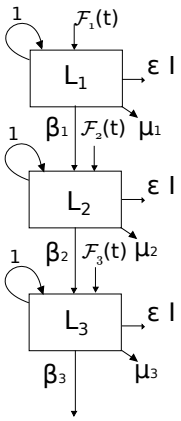

Figure 3: Larvae population model.

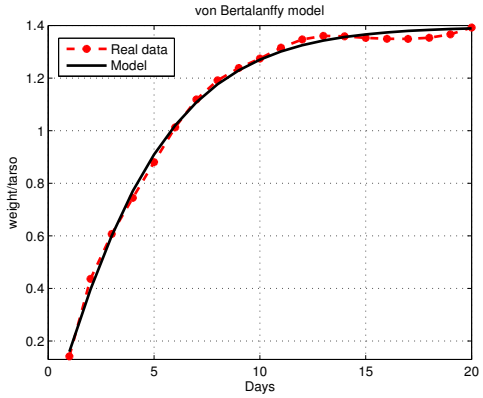

Figure 4: Von Bertalanffyt model for nestling weight/size relationship.

sinc(*i*) Research Center for Signals, Systems and Computational Intelligence (fich.unl.edu.ar/sinc)
L. López, A. Izquierdo, R. Manzoli, P. Beldoménico & L. Giovanini; "A myiasis model for Philornis torquans (Diptera: Muscidae) and Pitangus sulphuratus (Passeriformes: Tyrannidae)"
Ecological Modelling, Vol. 328, pp. 62-71, may, 2016.

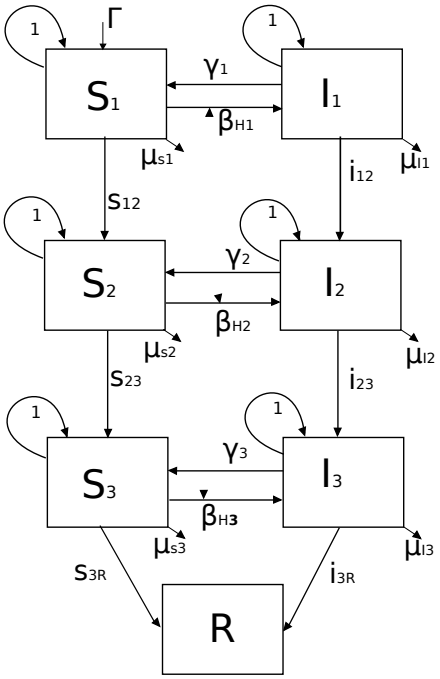

Figure 5: Nestlings population model.

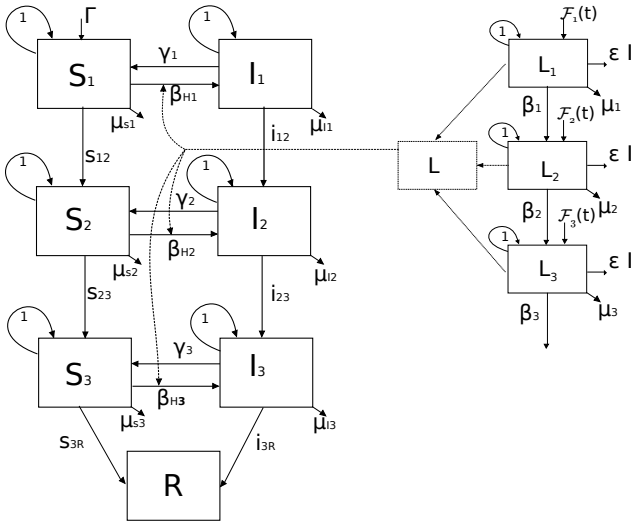

Figure 6: Myiasis model: larvae population model and nestlings population model join together.

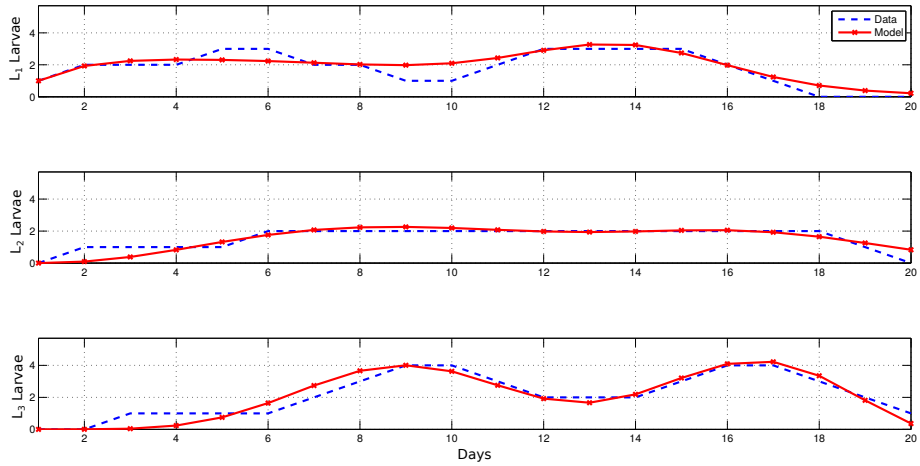

Figure 7: Optimized larvae population model temporal dynamics.

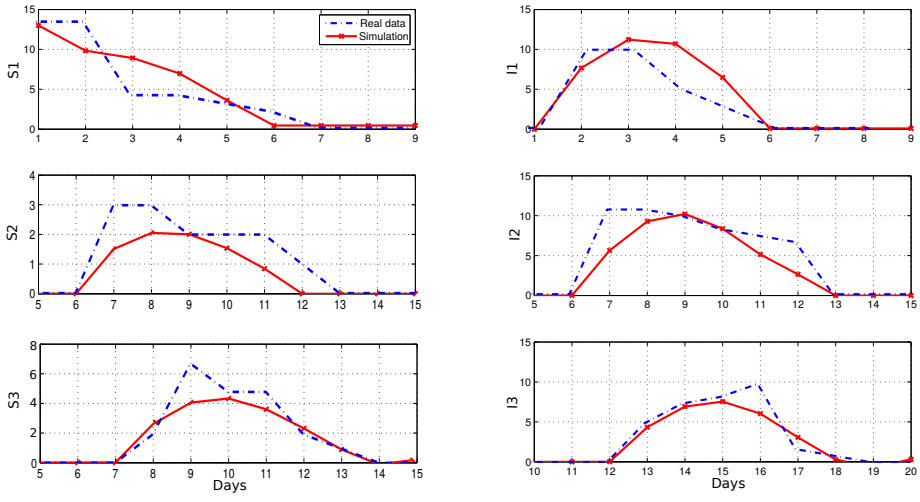

Figure 8: Optimized nestling population model temporal dynamics.

sinc(*i*) Research Center for Signals, Systems and Computational Intelligence (fich.unl.edu.ar/sinc)
L. López, A. Izquierdo, R. Manzoli, P. Beldoménico & L. Giovanini; "A myiasis model for Philornis torquans (Diptera: Muscidae) and Pitangus sulphuratus (Passeriformes: Tyrannidae)"
Ecological Modelling, Vol. 328, pp. 62-71, may, 2016.

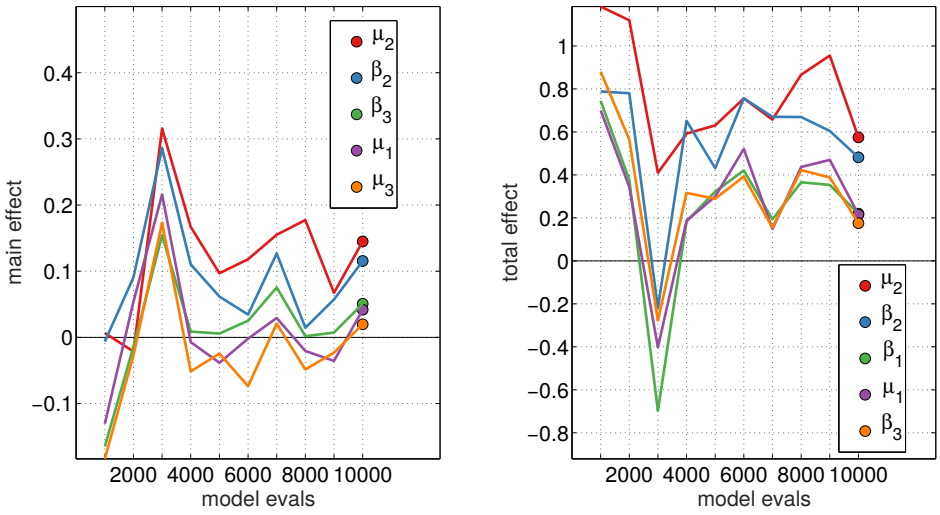

Figure 9: Global Sensitivity Analysis for Philornis model parameters.

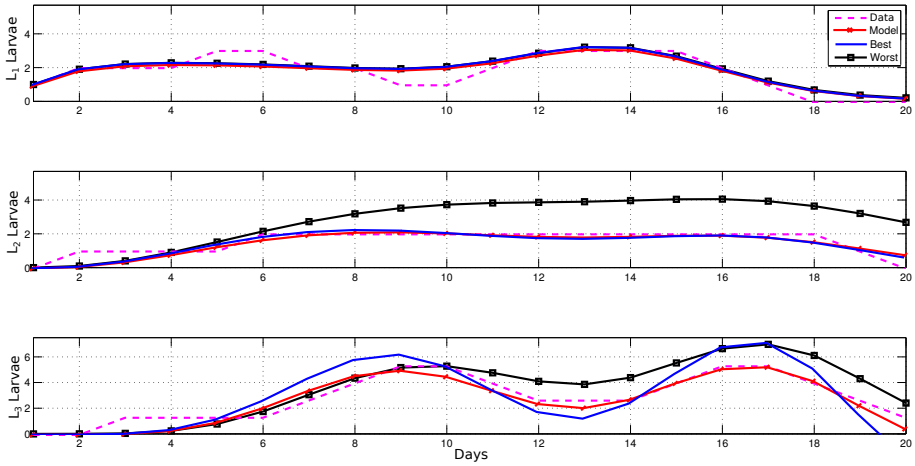

Figure 10: Comparison of the best and worst result of the GSA, the optimized model and the real data for the larvae population

sinc(*i*) Research Center for Signals, Systems and Computational Intelligence (fich.unl.edu.ar/sinc)
L. López, A. Izquierdo, R. Manzoli, P. Beldoménico & L. Giovanini; "A myiasis model for Philornis torquans (Diptera: Muscidae) and Pitangus sulphuratus (Passeriformes: Tyrannidae)"
Ecological Modelling, Vol. 328, pp. 62-71, may, 2016.

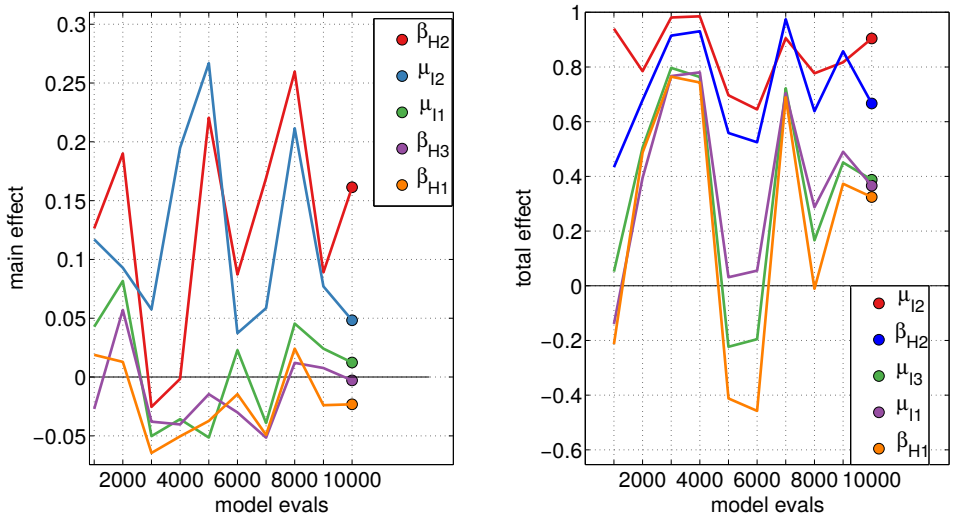

Figure 11: Global Sensitivity Analysis for Pitangus model parameters

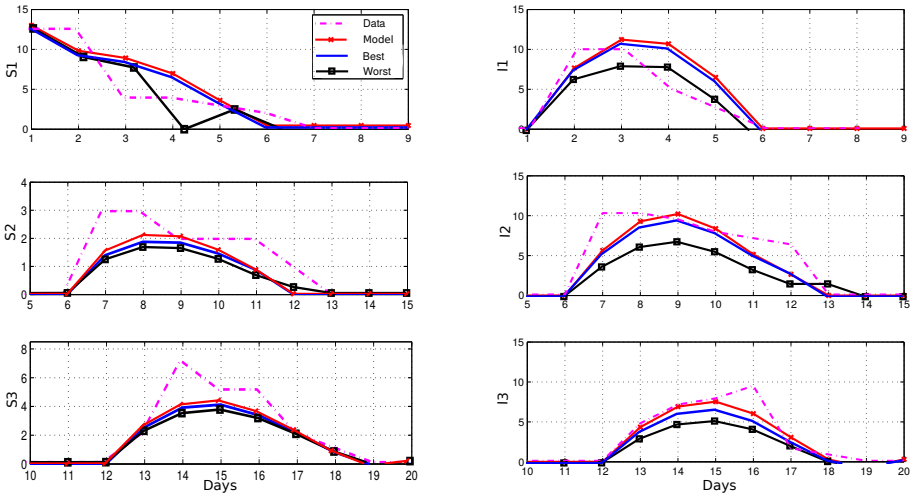

Figure 12: Comparison of the best and worst result of the GSA, the optimized model and the real data for the nestlings population

Appendix A. Model parameters

Parameters			
k_1	2.4512	σ_1	4.9510
β_1	0.4828	μ_1	1.9249
k_2	2.6875	σ_2	1.4422
ε	0.0022	a	0.0100
β_2	1.2422	μ_2	0.5115
β_3	1.2149	μ_3	0.4885
k_3	0.1570	σ_3	2.6170
k_4	0.5013	σ_4	0.0064

Table A.3: Larval model parameters

Parameters			
b_{s1}	0.4704	μ_{s1}	0.1702
β_{H1}	0.6353	b_{I1}	0.5961
μ_{I1}	0.2436	γ_1	0.9407
k	0.8094	s_{12}	0.1187
i_{12}	0.5948	b_{S2}	0.9657
μ_{S2}	0.5	β_{H2}	1.0345
s_{23}	1.3594	b_{I2}	0.46
μ_{I2}	0.6086	γ_2	1.8997
i_{23}	0.5	b_{S3}	0.3019
μ_{S3}	0.63	β_{H3}	0.5409
s_{3R}	1.1329	b_{I3}	0.7722
μ_{I3}	1.0128	γ_3	1.7838
i_{3R}	0.5177	θ	1.3667
c	1.1573		

Table A.4: Birds model parameters

References

[1] R. Wall, Ovine cutaneous myiasis: effects on production-control, Veterinary Parasitology 189 (1) (2012) 44–51.
[2] J. Guimarães, Myiasis in man and animals in the Neotropical Region. Bibliographic database, 1999.
[3] D. Wiedenfeld, G. Jiménez-Uzcátegui, Critical problems for bird conservation in the Galápagos Islands, Cotinga 29 (2008) 22–27.
[4] H. Serra, I. da Silva, P. de Arruda Mancera, L. Faria, C. Von Zuben, F. Von Zuben, S. dos Reis, W. Godoy, Stochastic dynamics in exotic and native blowflies: an analysis combining laboratory experiments and a two-patch metapopulation model, Ecological Research 22 (4) (2007) 686–695.
[5] R. Rosà, The importance of aggregation in the dynamics of host-parasite interaction in wildlife: A mathematical approach.
[6] P. Hudson, A. Dobson, Macroparasites: observed patterns in naturally fluctuating animal populations, Ecology of infectious diseases in natural populations 5 (1995) 144–176.
[7] R. M. Anderson, R. M. May, Regulation and stability of host-parasite population interactions: I. regulatory processes, The Journal of Animal Ecology (1978) 219–247.
[8] F. Gulland, The impact of infectious diseases on wild animal populations-a review, Ecology of infectious diseases in natural populations. Cambridge University Press, Cambridge (1995) 20–51.
[9] B. T. Grenfell, A. P. Dobson, Ecology of infectious diseases in natural populations, Vol. 7, Cambridge University Press, 1995.
[10] R. M. May, R. M. Anderson, Regulation and stability of host-parasite population interactions: Ii. destabilizing processes, The Journal of Animal Ecology (1978) 249–267.
[11] C. Kelehear, G. P. Brown, R. Shine, Size and sex matter: infection dynamics of an invading parasite (the pentastome raillietiella frenatus) in an invading host (the cane toad rhinella marina), Parasitology 139 (12) (2012) 1596–1604.
[12] S. Albon, A. Stien, R. Irvine, R. Langvatn, E. Ropstad, O. Halvorsen, The role of parasites in the dynamics of a reindeer population, Proceedings of the Royal Society of London B: Biological Sciences 269 (1500) (2002) 1625–1632.
[13] S. Paterson, J. Lello, Mixed models: getting the best use of parasitological data, Trends in parasitology 19 (8) (2003) 370–375.
[14] C. S. Gokhale, A. Papkou, A. Traulsen, H. Schulenburg, Lotka–volterra dynamics kills the red queen: population size fluctuations and associated stochasticity dramatically change host-parasite coevolution, BMC evolutionary biology 13 (1) (2013) 254.
[15] K. White, B. Grenfell, R. Hendry, O. Lejeune, J. Murray, Effect of seasonal host reproduction on host-macroparasite dynamics, Mathematical biosciences 137 (2) (1996) 79–99.
[16] M. Begon, R. Bowers, Beyond host-pathogen dynamics, Ecology of infectious diseases in natural populations 7 (1995) 478.
[17] M. Woolhouse, A theoretical framework for the immunoepidemiology of helminth infection, Parasite Immunology 14 (6) (1992) 563–578.
[18] M. S. Couri, L. R. Antoniazzi, P. Beldomenico, M. Quiroga, Argentine philornis meinert species (diptera: Muscidae) with synonymic notes, Zootaxa 2261 (5262) (2009) 77132.
[19] R. Dudaniec, S. Kleindorfer, Effects of the parasitic flies of the genus *Philornis* (Diptera: Muscidae) on birds, Emu 106 (1) (2006) 13–20.
[20] M. Couri, Myiasis caused by obligatory parasites. Ia. *Philornis* Meinert (Muscidae), JH Guimarães & N. Papavero, Myiasis in man and animals in the Neotropical Region. Bibliographica database. Pleaide, São Paulo (1999) 51–70.
[21] B. Fessl, S. Kleindorfer, S. Tebbich, An experimental study on the effects of an introduced parasite in Darwin's finches, Biological Conservation 127 (1) (2006) 55–61.
[22] L. Antoniazzi, D. Manzoli, D. Rohrmann, M. Saravia, L. Silvestri, P. Beldomenico, Climate variability affects the impact of parasitic flies on argentinean forest birds, Journal of Zoology 283 (2) (2011) 126–134.
[23] B. Young, Effects of the parasitic botfly *Philornis carinatus* on nestling House wrens, *Troglodytes aedon*, in Costa Rica, Oecologia 93 (2) (1993) 256–262.
[24] W. Arendt, *Philornis* ectoparasitism of pearly-eyed thrashers. i. impact on growth and development of nestlings, The Auk (1985) 270–280.
[25] W. Arendt, *Philornis* ectoparasitism of pearly-eyed thrashers. ii. effects on adults and reproduction, The Auk (1985) 281–292.
[26] L. Segura, J. Reboreda, Botfly parasitism effects on nestling growth and mortality of Red-crested Cardinals, The Wilson Journal of Ornithology 123 (1) (2011) 107–115.
[27] M. Quiroga, J. Reboreda, Lethal and sublethal effects of botfly (*Philornis seguyi*) parasitism on House wren nestlings, The Condor 114 (1) (2012) 197–202.
[28] D. E. Manzoli, L. R. Antoniazzi, M. J. Saravia, L. Silvestri, D. Rorhmann, P. M. Beldomenico, Multi-level determinants of parasitic fly infection in forest passerines, PLOS ONE 8 (7) (2013) e67104.
[29] N. Lester, B. Shuter, P. Abrams, Interpreting the von bertalanffy model of somatic growth in fishes: the cost of reproduction, Proceedings of the Royal Society of London. Series B: Biological Sciences 271 (1548) (2004) 1625–1631.
[30] K. Deb, A. Pratap, S. Agarwal, T. Meyarivan, A fast and elitist multiobjective genetic algorithm: Nsga-ii, Evolutionary Computation, IEEE Transactions on 6 (2) (2002) 182–197.
[31] C. R. Houck, J. A. Joines, M. G. Kay, A genetic algorithm for function optimization: a matlab implementation, NCSU-IE TR 95 (09).
[32] M. J. Powell, A fast algorithm for nonlinearly constrained optimization calculations, in: Numerical analysis, Springer, 1978, pp. 144–157.
[33] R. H. Byrd, J. C. Gilbert, J. Nocedal, A trust region method based on interior point techniques for nonlinear programming, Mathematical Programming 89 (1) (2000) 149–185.
[34] K. A. Dowsland, J. M. Thompson, Simulated annealing, in: Handbook of Natural Computing, Springer, 2012, pp. 1623–1655.
[35] P. E. Gill, E. Wong, Sequential quadratic programming methods, in: Mixed integer nonlinear programming, Springer, 2012, pp. 147–224.
[36] F. Pianosi, F. Sarrazin, T. Wagener, A matlab toolbox for global sensitivity analysis, Environmental Modelling & Software 70 (2015) 80–85.
[37] T. Homma, A. Saltelli, Importance measures in global sensitivity analysis of nonlinear models, Reliability Engineering & System Safety 52 (1) (1996) 1–17.
[38] A. Saltelli, M. Ratto, T. Andres, F. Campolongo, J. Cariboni, D. Gatelli, M. Saisana, S. Tarantola, Global sensitivity analysis: the primer, John Wiley & Sons, 2008.

sinc(*i*) Research Center for Signals, Systems and Computational Intelligence (fich.unl.edu.ar/sinc)
L. López, A. Izquierdo, R. Manzoli, P. Beldoménico & L. Giovanini; "A myiasis model for Philornis torquans (Diptera: Muscidae) and Pitangus sulphuratus (Passeriformes: Tyrannidae)"
Ecological Modelling, Vol. 328, pp. 62-71, may, 2016.